International Journal of Environmental Sciences
ISSN: 2229-7359
Vol. 11 No. 17s, 2025
https://theaspd.com/index.php

Synergistic Effect Of Ceftazidime-Loaded Silver Nanoparticles Against Multidrug-Resistant Pseudomonas Aeruginosa Isolated From Humans And Cats

Aws D.A. Al-Jabbari[1], Al-Zubaidy Ibrahim A.H.[2]
[1,2]Zoonotic Diseases Research Unit, College of Veterinary Medicine, University of Baghdad, Baghdad, Iraq
aws.abd2309m@covm.uobaghdad.edu.iq[1], ibrahim_hussien2000@covm.uobaghdad.edu.iq[2]

Abstract
This study investigates the synergistic antibacterial effects of ceftazidime-loaded silver nanoparticles (AgNPs-CAZ) on P. aeruginosa recovered from humans as well as cats. A total of 103 clinical and veterinary samples (60 human, 43 cat) revealed 12 isolates (9 human, 3 cat), as confirmed by biochemical and VITEK 2 analysis. All isolates produced biofilms. Silver nanoparticles were prepared using a chemical reduction method, then conjugated with ceftazidime and characterized using UV-Vis, DLS, FTIR, and FESEM. The macrodilution tube method was used to determine MICs, and antibacterial activity was further tested using agar well diffusion. Following conjugation, ceftazidime MICs were lowered 32-fold in human isolates and 8-fold in cat isolates. FICI analysis showed additive effects (0.812 in humans, 0.515 in cats). Moreover, the AgNPs-CAZ combination showed increased inhibition zones than either drug alone, demonstrating enhanced antibacterial action. These results suggest that AgNPs-CAZ conjugates may enhance antibiotic activity and could be a viable option for treating resistant P. aeruginosa infections.
Keywords: *AgNPs, AgNPs-CAZ, Minimum inhibitory concentrations, Antibiotic resistance, Iraq*

INTRODUCTION

Pseudomonas aeruginosa, an opportunistic bacterium, can induce life-threatening infections not only in humans and animals, especially immunodeficient ones such as cats [1, 2]. P. aeruginosa is well known to generate biofilms and virulence factors [3, 4], which enable P. aeruginosa to escape from the immune system and set up chronic infections [5-7]. P. aeruginosa has multidrug resistance and there are various mechanisms by which P. aeruginosa resistance could be acquired such as, efflux pumps, low permeability of outer membrane, antibiotic hydrolyzing enzymes. This makes it more difficult to cure [8, 9]. Overuse of antibiotics allows bacteria to become more resistant to them, a major threat to public health globally. Therefore, new and efficient antibacterial solutions that could be applied for the antibiotic-resistant P. aeruginosa have to be found [10, 11]. Nanoparticles (NPs) emerge as new tools against bacterial resistance [12, 13]. For example, silver nanoparticles (AgNPs) can cause bacteria to die by disrupting their cell membrane or cell wall, rather than penetrating the cell. Also, AgNPs have been used with common antibiotics to improve their working against bacteria synergistically [14, 15]. AgNPs promote the effectiveness of antibiotics by directing them to the various sites, leading to lower doses and fewer negative side effects [16, 17].

MATERIALS AND METHODS

Collection of Samples

From 3 November 2024 to 3 January 2025, 103 swab samples were collected in Baghdad City, from the Baghdad Medical City (Burns Center) and various veterinary clinics. Of these, 60 were from humans and 43 from Cats. Sterile gloves were used to prevent contamination. Transport medium swabs were collected from both genders, ages 2 to 78 years for humans and 3 months to 7 years for animals. The samples were sent to the Microbiological Laboratory at the College of Veterinary Medicine, University of Baghdad. MacConkey, Cetrimide, and Blood agar media were used to culture the samples for bacterial isolation and preliminary identification [18].

Preparation of Culture Media

The culture media, including MacConkey, Cetrimide, and blood agar, were prepared per the manufacturer's instructions and maintained under refrigerated conditions until needed.

Phenotypic Characterization of Pseudomonas aeruginosa

To observe the morphological aspects of colonies, including form, size, color, odor, and pigment production. After culturing P. aeruginosa on MacConkey, Cetrimide, and blood agar, Gram staining was performed to evaluate their staining reaction, morphology, and cellular arrangement under the light microscope [18,19,20].

Biochemical and Vitek2-based Identification of P. aeruginosa

Preliminary identification relied on conventional biochemical tests such as oxidase and catalase, MR-VP, citrate, TSI, urease, SIM, phenylalanine deamination, and gelatin liquefaction tests, performed [18]. The VITEK 2 system was utilized for final confirmation, following the protocol provided by the manufacturer (BioMérieux, France) [21, 22].

Maintenance and Preservation of P. aeruginosa

According to [23], in an Eppendorf tube, 1 mL of the bacterial culture was combined with an equivalent volume of Brain Heart Infusion (BHI) broth that contained 20% glycerol. The mixture was then vortexed vigorously and kept at -20°C to preserve it.

Biofilm Formation Assay

The tube adherence method, as previously outlined by [24, 25, 26], was employed to evaluate biofilm formation by P. aeruginosa isolates. Biofilm production was evaluated visually by seeing stained residues around the inner walls of the test tubes.

Synthesis of Silver Nanoparticles

Silver nanoparticles (AgNPs) were prepared using a modified chemical reduction protocol. In brief, 4 mM of $AgNO_3$ and 0.2 mM of PVP were dissolved in 100 mL of deionized water and magnetic stirred until a clear solution was obtained. Subsequently, 0.4 mM TSC (in 100 mL water) solution was drop-wise introduced within 30 min. The solution was then heated at 80°C for 2 h and stirred (350 rpm). The color change to yellow showed the formation of AgNPs. The cold solution was kept in dark capped glass vials at 4°C [27].

Loading of Ceftazidime onto Silver Nanoparticles (AgNPs)

A modified procedure by [28] was used. The AgNPs solution was ultrasonicated (40 kHz, 150–200 W) for 30–45 min at 42 °C in order to maintain homogeneity. Ceftazidime was stirred at 100 to 200 rpm, and AgNPs were added dropwise. Afterwards, the drug adsorption was realized at room temperature for 1 h under agitation. The AgNPs–CAZ conjugate was stored at 4 °C until use.

Characterization of AgNPs and AgNPs-CAZ

The optical properties of AgNPs and AgNPs-CAZ were evaluated by UV-Vis spectrophotometry (Model 1200, Shimadzu, Kyoto, Japan) from 200 to 1000 nm. Morphological and surface images were observed by Field Emission Scanning Electron Microscopy (FESEM) (FEI, Thermo Fisher Scientific, USA). Determination of functional groups and verification of the formation of nanoparticles FTIR analysis was performed using an IFS 48 spectrometer (Bruker, Germany range 4000–400 cm^{-1}). The hydrodynamic size distribution of the NPs was determined using Dynamic Light Scattering (DLS) [29, 30, 31]. Both AgNPs and ceftazidime loaded AgNPs were analysed in separate analyses.

Determination of MIC and FICI

The MICs of ceftazidime (CAZ), silver nanoparticles (AgNPs), and their combination (AgNPs–CAZ) were conducted using the broth macrodilution assay under standardized CLSI guidelines [32], with minor modifications. After incubation, 20 µL of triphenyl tetrazolium chloride (0.5%) solution was added to the ceftazidime tubes, then incubated for 30 minutes to help in visually checking for bacterial growth. The MIC is the minimum concentration of an antimicrobial agent needed to inhibit the growth of a microorganism. To determine the interaction between CAZ and AgNPs-CAZ, the formula used to calculate the fractional inhibitory concentration index (FICI) values as follows: FICI = (MIC of CAZ in Mix / MIC of CAZ alone) + (MIC of AgNPs in Mix / MIC of AgNPs alone). If the FICI value is ≤ 0.5, meaning a synergetic effect, more than 0.5 < and less than ≤ 1, meaning an additive effect, and if the value 1 < FICI ≤ 2, meaning an Indifferent effect, and if the value is more than > 2, it means an antagonistic effect [33].

Assessment of Antimicrobial Activity

Antibacterial activity of AgNPs and this of ceftazidime and ceftazidime loaded nanoparticles was assessed using the agar well diffusion technique [27, 34, 35]. Synergy was considered present when the inhibition

zone produced by ceftazidime-loaded silver nanoparticles (AgNPs–CAZ) exceeded the larger inhibition zone obtained by either ceftazidime (CAZ) or silver nanoparticles (AgNPs) alone by at least 2 mm.

Ethical Approval

We confirm that this study was approved by the Ethics Committee of the College of Veterinary Medicine, University of Baghdad (Approval No. P-G/1337, dated 2 June 2025). No experiments were performed on animals. We only collected swab samples from cats during regular clinical visits, and the collection process followed ethical and professional guidelines.

Statistical Analysis

We used the 2019 edition of SPSS to look at how different factors affected the observed proportions. We used the Chi-square test to check for statistical significance at 95% and 99% confidence levels [36].

RESULTS

Pseudomonas aeruginosa Isolation and Validation

Twelve Pseudomonas aeruginosa isolates were found in the 103 samples that were examined. Three of these isolates were from cats, while nine were from human clinical samples. The cultural and microscopic characteristics of the isolates were consistent with Pseudomonas aeruginosa. On MacConkey agar, the colonies appeared pale due to the absence of lactose fermentation. In contrast, growth on Cetrimide agar, a selective medium, produced yellowish-green, smooth, and mucoid colonies, supporting the selective growth of P. aeruginosa while inhibiting other bacterial species. On blood agar, colonies displayed beta-hemolysis and had a gray to grayish-white appearance (Figure 1).Microscopically, the bacterial cells were Gram-negative rods, according to [37]. Figure 2 (microscopic appearance).

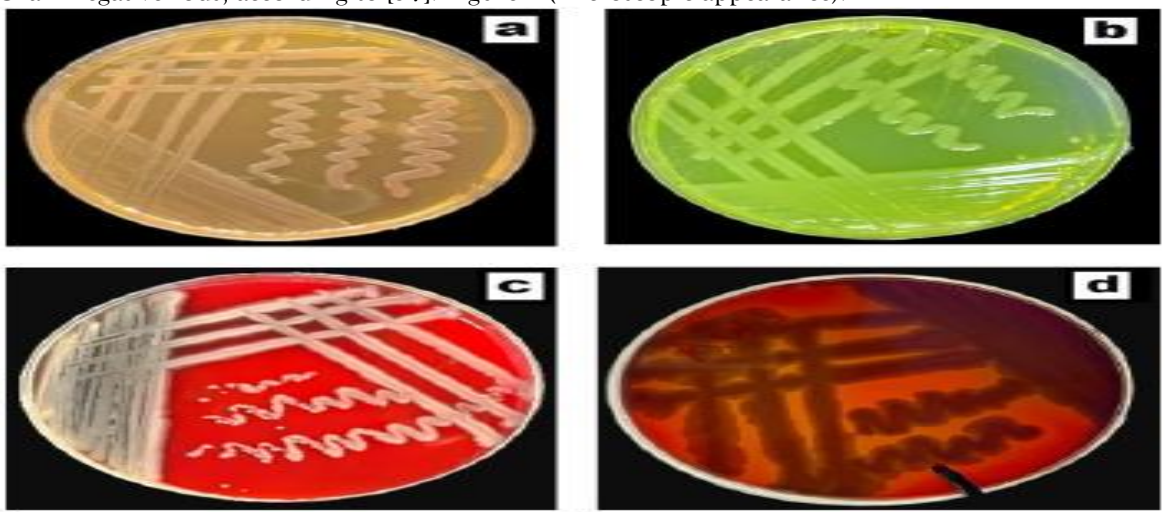

Figure 1: Colonies of Pseudomonas aeruginosa on different bacteriological media: (a) MacConkey agar, (b) Cetrimide agar, grayish-white colonies on blood agar, and (D) beta-hemolysis on blood agar

Figure 2: P. aeruginosa on Gram stain (100× oil immersion)

The biochemical identification of isolates indicated results aligned with P. aeruginosa. Oxidase and catalase (a), as well as gelatin hydrolysis (b), yielded positive results. TSI (c) exhibited K/K without the presence of gas or H_2S. SIM (d) exhibited positive motility and negative indole. Citrate (e) tested positive, although MR/VP (f), urease (g), and phenylalanine deaminase (h) all tested negative, as illustrated in

Figure 3. For further assurance, we used the VITEK 2 system, which correctly identified P. aeruginosa in a variety of samples (see Table 1 for details).

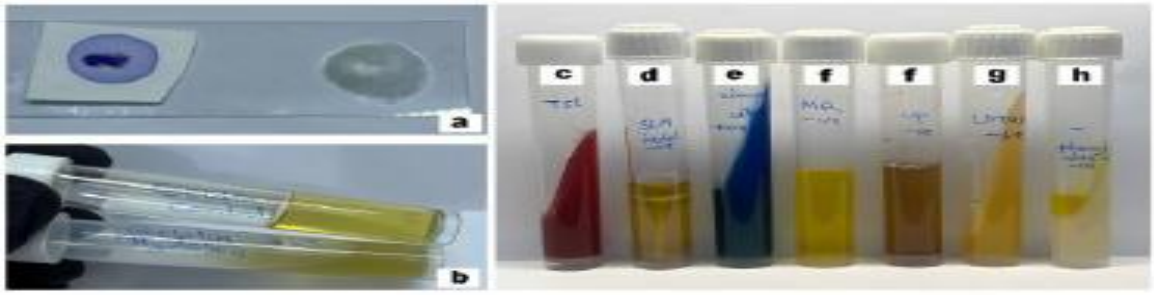

Figure 3: Biochemical test findings for P. aeruginosa isolates

Table 1: VITEK 2 system-based identification of P. aeruginosa isolates

No	Host	Sample	No of Isolates	Probability (%)
1	Humans	Burns	9	93-99 %
2	Cats	Wound	3	99 %
Total			14	

Biofilm Formation

The qualitative tube adherence approach showed that all of the Pseudomonas aeruginosa isolates have the biofilm-forming capability. It was suggested that the presence of a discolored coating on the inside of the tubes meant that biofilm was forming. Table 2 and Figure 4 show the full results.

Table 2: Positive biofilm production of P. aeruginosa isolates

No	Source of Isolates	Number of Isolates	Biofilm Production (%)
1	Human	9	100
2	Cat	3	100
	Total	14	---
	P-value	1.00 NS	---
NS: Non-Significant.			

Figure 4: Positive results of P. aeruginosa biofilm forming ability (tube adherence method)

Synthesis and characterization of silver nanoparticles and their conjugates with ceftazidime

Silver nanoparticles generated through chemical reduction result in a unique golden-yellow colour. This comes from the surface plasmon resonance (SPR), which is a common phenomenon in silver nanoparticles [38]. After ceftazidime loading, the golden-yellow intensity faded a little bit without any clear aggregation, which showed that ceftazidime had been successfully loaded onto the AgNPs (Figure 5).

Figure 5: Chemically synthesized AgNPs and AgNPs-CAZ

UV-Visible spectroscopy

When the colour shifted to golden-yellow, a clear SPR peak at 407 nm in the UV–Vis spectrum showed that silver nanoparticles had formed. After loading ceftazidime, the spectra showed two peaks at 254 nm and 414 nm. These peaks show the ceftazidime absorbance and the SPR of the loaded nanoparticles, respectively (Figure 6).

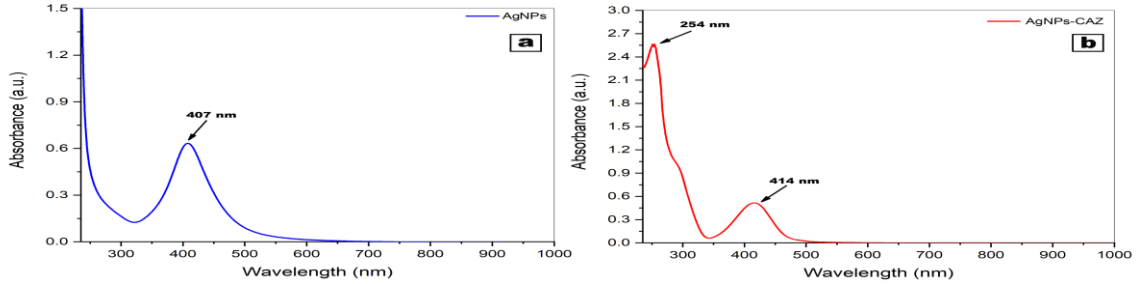

Figure 6: Uv-Vis spectroscopy of (a) AgNPs, (b) AgNPs-CAZ

Dynamic Light Scattering (DLS)

DLS analysis showed that AgNPs were evenly spread out, with a PDI of 0.246 and a particle size of 19.8 nm. After loading ceftazidime, the size increased to 28.4 nm and the PDI to 0.321, which shows that the surface changed and the heterogeneity was moderate (Figure 7).

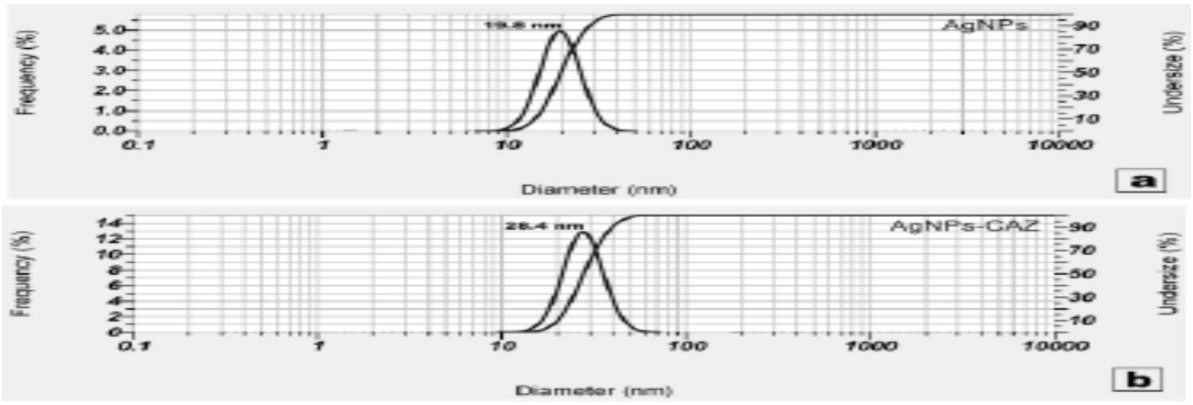

Figure 7: DLS Analysis of (a) AgNPs, (b) AgNPs-CAZ

Fourier Transform Infrared Spectroscopy (FTIR)

The FTIR analysis of AgNPs showed clear bands at 3414 cm^{-1} (O–H/N–H), 2949–2889 cm^{-1} (C–H), and strong carbonyl peaks at 1737–1680 cm^{-1} (Figure 8). This suggested that stabilizers like PVP had successfully capped the particles. After loading ceftazidime, the carbonyl peaks moved a lot (to 1768 and 1651 cm^{-1}), and the fingerprint regions changed slightly (Figure 8). This showed that the medication interacted with the nanoparticles and changed the structure of the surface slightly.

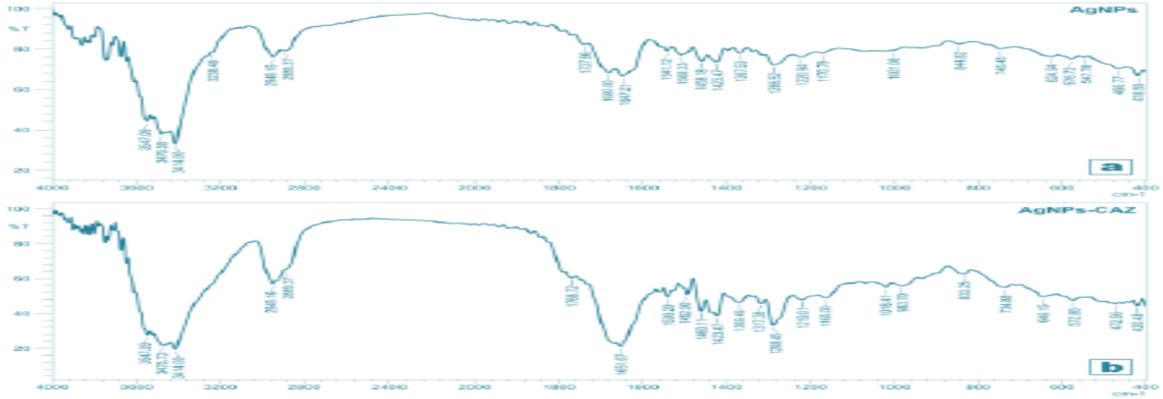

Figure 8: FTIR analysis showing characteristic peaks for (a) AgNPs and (b) AgNPs-CAZ

Field Emission Scanning Electron Microscopy (FESEM)

FESEM images indicated that unmodified AgNPs were equally distributed, spherical, and well-dispersed with modest diameters. Following the loading of ceftazidime, the particles retained their spherical shape but were marginally larger and denser, suggesting effective surface coverage by the antibiotic (Figure 9).

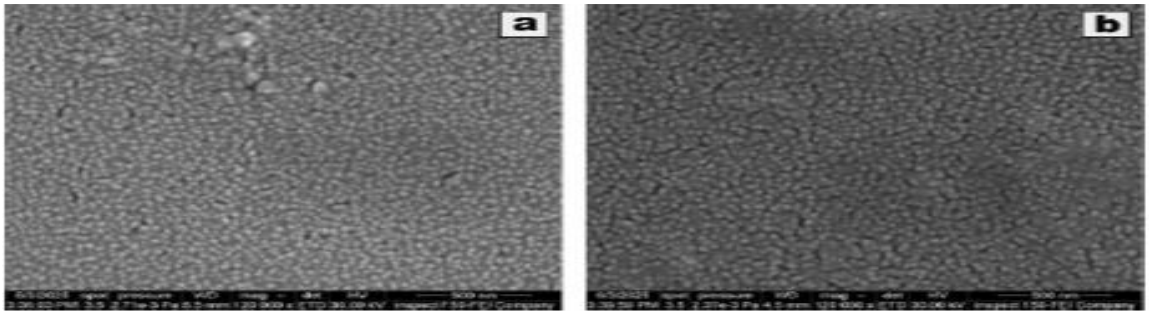

Figure 9: FESEM images of (a) AgNPs, and (b) AgNPs-CAZ

Minimum Inhibitory Concentration (MIC) and FICI Values

Ceftazidime alone resulted in an MIC of 512 µg/mL for the human isolate as well as 64 µg/mL for the cat isolate (Figure 10). Figure 11 shows that silver nanoparticles (AgNPs) had similar MIC values (8 µg/mL) in samples recovered from humans and cats. Loading ceftazidime to AgNPs lowered the MIC values to 16/6.25 µg/mL (CAZ/AgNPs) for human isolates and 8/6.25 µg/mL for cat isolates, which means the antibacterial activity was enhanced (Figure 12).

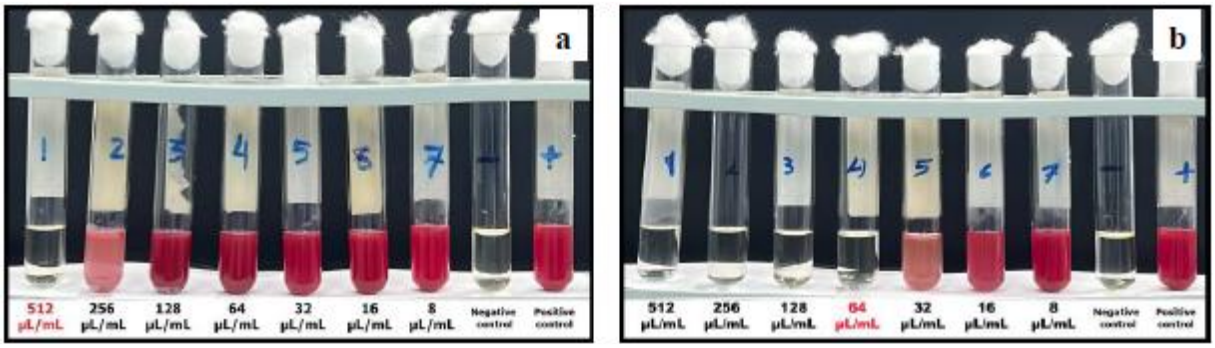

Figure 10: MIC of ceftazidime (CAZ) for (a) Human, (b) Cat isolates visualized using triphenyl tetrazolium chloride (TTC)

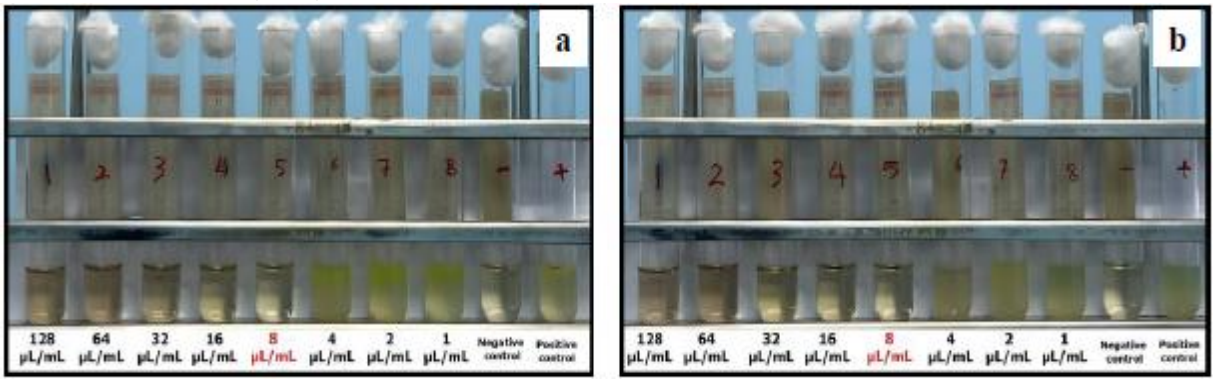

Figure 11: MIC of AgNPs for (a) Human, (b) Cat isolates

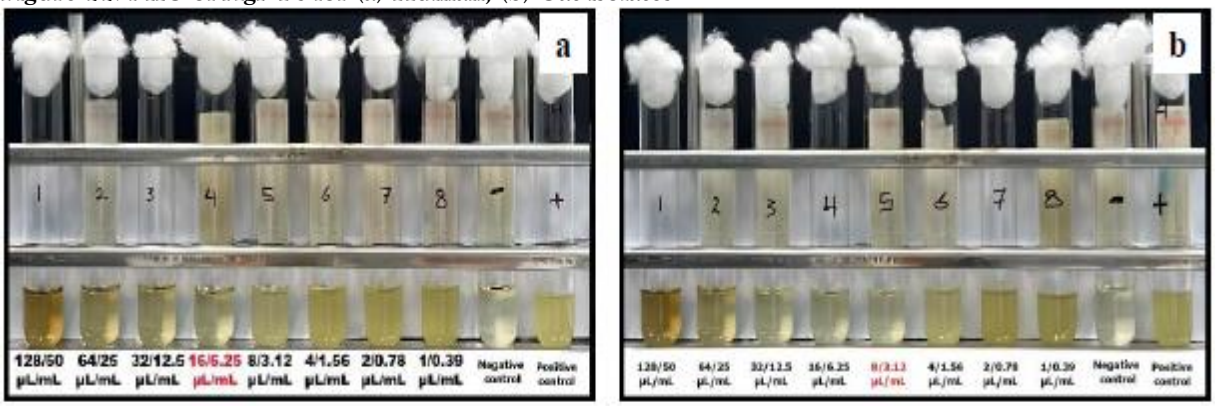

Figure 12: MIC of AgNPs-CAZ for (a) Human, (b) Cat isolates

As shown in Table 3, both samples recovered from human (0.812) and cat (0.515) isolates had additive effects on the FICI values. This proves that the antibacterial efficacy of the combined therapy is increased.

Table 3: FICI Values and Interaction Interpretation

Samples	MIC of Ceftazidime	MIC of AgNPs	MIC of AgNPs-CAZ	FICI (Interpretation)
Human	512	8	16/6.25	0.812 (Additive)
Cat	64	8	8/3.12	0.515 (Additive)

Agar Well Diffusion Test for Antibacterial Activity Assessment

For both the human and feline isolates, the inhibition zones measured 29.36 mm and 19.03 mm, respectively, when the AgNPs-CAZ combination was compared to ceftazidime and AgNPs alone. It is revealed that the antibacterial activities are enhanced remarkably after the conjugation. A visual aid of these inhibitory zones based on the comparative diameters is presented in Figure 13.

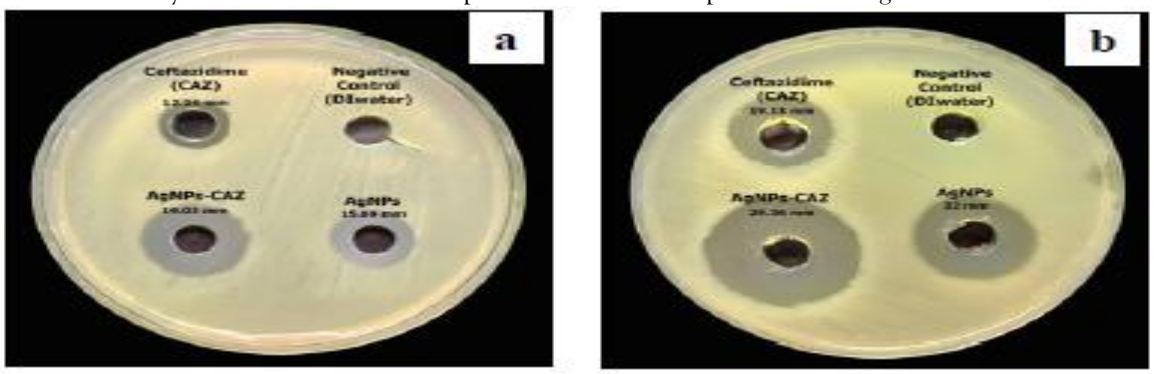

Figure 13: Agar well diffusion showing zones of inhibition for samples from (a) human and (b) cat isolates

DISCUSSION

Pseudomonas aeruginosa Isolation and Identification

We identified 9 samples of human burns and 3 samples of cat wounds. We discovered P. aeruginosa in 15% of human burn samples and 7% of cat wound samples. [39, 40] found rates as high as 62%, which is not what these results show. We get 11.7% for both human burns and cat wounds, which is different from what [41] discovered in Samawa (8.2%) and [42] found in samples of cat wounds (20%). There are a few things that could cause the isolation rate to be different, like where the person lives, whether or not they have been around antibiotics previously, and how clean the area is. All 12 isolates presented with normal growth characteristics including no lactose fermentation on MacConkey agar (pale colonies), smooth yellow green colonies with fruity smell on Cetrimide agar, β-hemolytic growth on blood agar. These results are consistent with [43]. in light microscope, and that were stained red as a Gram-negative form under a microscope, consistent with [44]. The biochemical test results in this work were similar to those of P. aeruginosa which was consistent with [39]. Subsequently, further identification was confirmed by the VITEK 2 system whose findings were similar to those reported in [44].

Biofilm formation

We discovered that all five strains of Pseudomonas aeruginosa that we got from humans and cats could make biofilms (100%). We found that burns on humans and wounds on cats may all generate biofilm. [45] found very similar results, showing that 100% of the biofilm-forming potential was also present. [46] found an 89% of the P. aeruginosa collected from cats could make biofilms. [47] found that 93% of the isolates from both humans and animals could also make biofilms. These two studies accord with part of what we discovered, though. It's known that biofilm formation helps Pseudomonas aeruginosa survive and resist antibiotics in both humans and animals.

Structural and Functional Analysis of AgNPs and Their Conjugates

We noticed a unique surface plasmon resonance (SPR) signal at 407 nm in the UV–Visible absorption spectra of AgNPs. This is in line with [48], who record a peak at 408 nm. The peak moved to 414 nm in the AgNPs–CAZ conjugate, which means that the ceftazidime was loaded successfully. This is like what was recorded by [27], where the SPR changed from 405 to 415 nm following loading with ciprofloxacin.

There was another signal at 254 nm that verified the presence of ceftazidime (Figure 6). The hydrodynamic diameter of AgNPs was determined to be 19.8 nm by DLS measurements, which is quite close to the 18 nm reported by [49]. The size increased to 28.4 nm after ceftazidime loading, which is the same as [49], who record 27.9 nm in drug-loaded AgNPs. This growth confirms that the ceftazidime has been adsorbed onto the surface and that the conjugation process has been successful. FTIR analysis of AgNPs showed unique peaks at 3414 cm^{-1} (O-H/N-H), 2949-2889 cm^{-1} (C-H), and carbonyl bands at 1737.86 and 1680.00 cm^{-1}. These results are comparable to what [27] found with galactose-assisted AgNPs. When ceftazidime was loaded, the peaks shifted (for example, from 1737.86 to 1768.72 cm^{-1} and from 1680.00 to 1651.07 cm^{-1}), the bands got wider, and the intensity went down. These changes in the spectrum suggest a strong interaction with the antibiotic, which is in line with the studies [49, 47]. The FESEM analysis of the AgNPs showed that the particles were well-dispersed, spherical, had a consistent shape, and had smooth surfaces. This was similar to the results for unloaded AgNPs as reported by [27]. After loading with ceftazidime, the particles kept their spherical shape but became rougher and thicker, which suggests that they covered the surface well. These traits are consistent with [27], who record the same results with ciprofloxacin-loaded AgNPs, which had a denser surface without clumping. The form that stays the same before and after loading shows that the medicine sticks well while keeping the nanoparticles' integrity.

MIC and FICI Findings

Our findings of MIC for ceftazidime alone were 512 µg/mL for the human isolate and 64 µg/mL for the cat isolate. Additionally, for AgNPs, both human and animal isolates were 8 µg/mL. After loading ceftazidime with AgNPs, the MIC was reduced to 16/6.25 µg/mL for humans as well as 8/6.25 µg/mL for cats. Our results mean that ceftazidime decreased by 32-fold for humans and 8-fold for cats. Our results are in agreement with [50], who also reported a 2-9-fold decrease in MIC when loaded ceftazidime with AgNPs. Interaction between silver nanoparticles and antibiotic was determined by the FICI, if the FICI value is ≤ 0.5, meaning a synergetic effect, more than $0.5 <$ and less than ≤ 1, meaning an additive effect, and if the value $1 <$ FICI ≤ 2, meaning an Indifferent effect, and if the value is more than > 2, it means an antagonistic effect. Our results show an additive effect, which is partially in agreement with [50], who found a synergistic effect when ceftazidime was loaded with AgNPs in 76% of the P. aeruginosa. These findings support that AgNPs enhance the antibacterial effect of antibiotics.

Agar Well Diffusion Test

When we used AgNPs–CAZ on human and cat isolates, the inhibition zones expanded to 35.33 mm and 31.66 mm, respectively. There were more zones than the 16 mm and 14 mm zones that were found with ceftazidime alone and the 18 mm and 17 mm zones that were seen with AgNPs alone. Our results are in agreement with [27], who reported that adding AgNPs to ciprofloxacin generated the same increase in the size of inhibitory zones: 31.00 mm for A. baumannii, 32.66 mm for S. marcescens, and 35.33 mm for S. aureus. These results back up the hypothesis that nanoparticles with antibiotics can help antibiotics perform better against bacteria by going deeper into the body and concentrating the antibiotic where the sickness is.

REFERENCES

1. Qin, S., Xiao, W., Zhou, C., Pu, Q., Deng, X., Lan, L., Liang, H., Song, X., and Wu, M. (2022). Pseudomonas aeruginosa: pathogenesis, virulence factors, antibiotic resistance, interaction with host, technology advances and emerging therapeutics. Signal Transduction and Targeted Therapy, 7(1), 199.

2. Razook, B. R. F., Al-ani, A. N., and Mahmood, M. M. (2020). Hematological picture of rabbits immunized with Pseudomonas aeruginosa. The Iraqi Journal of Veterinary Medicine, 44(E0)), 64–68.

3. Hayashi, W., Izumi, K., Yoshida, S., Takizawa, S., Sakaguchi, K., Iyori, K., Minoshima, K., Takano, S., Kitagawa, M., and Nagano, Y. (2021). Antimicrobial resistance and type III secretion system virulotypes of Pseudomonas aeruginosa isolates from dogs and cats in primary veterinary hospitals in Japan: identification of the international high-risk clone sequence type 235. Microbiology Spectrum, 9(2), e00408-21.

4. Jasim, H., and Diwan, S. (2010). ISOLATION AND IDENTIFICATION OF CHOLESTEROLOXIDASE PRODUCING Pseudomonas Aeruginosa. Iraqi Journal of Science, 51(2), 284–289.

5. Al-Taee, H. S. R., Al-Samarraae, I. A. A., and Al-Ahmed, H. I. (2019). Antibiotic susceptibility and molecular detection of pseudomonas aeruginosa isolated from bovine mastitis. The Iraqi Journal of Veterinary Medicine, 43(2), 77–85.

6. Mahmood, A. N., and Aljobori, A. H. (2015). Isolation and identification of Pseudomonas aeruginosa from infected sheep and detection of phosolipase C (lecithinase). Iraqi J. Vet. Medicine, 39, 28–32.

7. Sarhan, S. R. (2017). Activity of isolated specific bacteriophage in treatment of chronic osteomyelitis induced by multiple

drug resistance Pseudomonas aeruginosa in Rabbits. The Iraqi Journal of Veterinary Medicine, 41(2), 146–156.
8. Langendonk, R. F., Neill, D. R., and Fothergill, J. L. (2021). The building blocks of antimicrobial resistance in Pseudomonas aeruginosa: implications for current resistance-breaking therapies. Frontiers in Cellular and Infection Microbiology, 11, 665759.
9. Sulaiman, S. D., and Abdulhasan, G. A. (2020). Curcumin as efflux pump inhibitor agent for enhancement treatment against multidrug resistant Pseudomonas aeruginosa isolates. Iraqi Journal of Science, 59–67.
10. Khleifat, K., Qaralleh, H., and Al-Limoun, M. (2022). Antibacterial activity of silver nanoparticles synthesized by aspergillus flavusand its synergistic effect with antibiotics. J. Pure Appl. Microbiol, 16(3), 1722–1735.
11. Otu, J. U., Edim, S. N., Ugor, S. O., and Obiaje, J. U. (2023). 16S Ribosomal Gene Sequencing, Phylogeny and Multidrug Resistance of Pseudomonas aeruginosa Isolated from Clinical Samples at a Tertiary Healthcare Facility in Nigeria. European Journal of Medical and Health Research, 1(3), 87–97.
12. Zou, W., McAdorey, A., Yan, H., and Chen, W. (2023). Nanomedicine to overcome antimicrobial resistance: Challenges and prospects. Nanomedicine, 18(5), 471–484.
13. Afolayan, J. S., Varney, A. M., Thomas, J. C., McLean, S., and Perry, C. C. (2025). A rapid microwave approach for 'one-pot'synthesis of antibiotic conjugated silver nanoparticles with antimicrobial activity against multi-drug resistant bacterial pathogens. Colloids and Surfaces B: Biointerfaces, 245, 114280.
14. Yang, N., Wu, T., Li, M., Hu, X., Ma, R., Jiang, W., Su, Z., Yang, R., and Zhu, C. (2025). Silver-quercetin-loaded honeycomb-like Ti-based interface combats infection-triggered excessive inflammation via specific bactericidal and macrophage reprogramming. Bioactive Materials, 43, 48–66.
15. Salih, A. N. A., and Eesa, M. J. (2017). Antibacterial ativity of biosynthesized silver nanoparticles against Pseudomonas aeruginosa in vitro: Ahmad NA Salih1 Orooba MS Ibrahim1 Mohammad J. Eesa2. The Iraqi Journal of Veterinary Medicine, 41(1), 60–65.
16. Asadpour, L., Bandari, M. A. M., and Masouleh, R. S. (2025). Amikacin-loaded selenium nanoparticles improved antibacterial and antibiofilm activity of amikacin against bovine mastitis-causing Staphylococcus aureus. Heliyon, 11(1).
17. Mohammed, A. S. A., Mourad, M. I., Alsewy, F. Z., and Azzam, N. F. A. E. M. (2021). Combination of silver nanoparticles with ineffective antibiotics against extended spectrum beta-lactamases producing isolates at Alexandria Main University Hospital, Egypt. Beni-Suef University Journal of Basic and Applied Sciences, 10, 1–8.
18. Tille, P. M., and Forbes, B. A. (2021). Bailey and Scott's Diagnostic Microbiology. St. Louis, Missouri. Elsevier.
19. Al-Mohammed, T. A., and Mahmood, H. M. (2024). Carbapenem resistance related with biofilm formation and pilin genes in clinical Pseudomonas aeruginosa isolates. Iraqi Journal of Pharmaceutical Sciences (P-ISSN 1683-3597 E-ISSN 2521-3512), 33(1), 72–78.
20. Jasim, S., and Hayyawi, S. M. (2025). Isolation and Detection of Biofilm Producing Pseudomonas aeruginosa from Suspected Urinary Tract Infections in Dogs and Its Resistance to Antibiotics. The Iraqi Journal of Veterinary Medicine, 49(1), 45–54.
21. Matrood, S. K., Abbas, I. J., and Al-Hello, M. F. (2025). Relationship Between Pseudomonas aeruginosa Infection and Some Physiological Parameter in Patients with UTIs. Basrah Researches Sciences, 51(1), 7.
22. Wadi, F. R., and Ali, M. K. (2025). Isolation and Antibiotic Sensitivity Testing of Pseudomonas aeruginosa Isolates from Patients with Chronic Suppurative Otitis Media in Baghdad. Ibn AL-Haitham Journal For Pure and Applied Sciences, 38(1), 27–36.
23. Willey, J. M., Sherwood, L. M., and Woolverton, C. J. (2008). Prescott, Harley, and Klein's microbiology. McGraw-Hill.
24. Reddy, C. M. S., and Ramnani, V. K. (2024). ASSESSMENT OF DISTINCTIVE DISCOVERIES STRATEGIES OF BIOFILM ARRANGEMENT IN URINARY CONFINES. Int J Acad Med Pharm, 6(5), 330–333.
25. Mohsenzadeh, A., Mohsenzadeh, H., Mohammadi, A., Panji, A., Mehranpour, R., Kamali, K., Aghasafi, M., Fereidouni, A., and Pourasgar, S. (2025). Synergistic effects of zinc oxide nanoparticles and Meropenem on biofilm formation in Pseudomonas aeruginosa. Cellular, Molecular and Biomedical Reports, 5(2), 121–134.
26. Vitharana, B. M., Wahalathantry, D. M., Gunasekara, S. P., Chathuranga, B. A. G., and Gunasekara, T. (2025). Biofilm formation and antimicrobial resistance of Enterobacteriaceae isolated from cancer patients with urinary tract infections. Sri Lankan Journal of Infectious Diseases, 15(2)
27. Ibraheem, D. R., Hussein, N. N., and Sulaiman, G. M. (2023). Antibacterial activity of silver nanoparticles against pathogenic bacterial isolates from diabetic foot patients. Iraqi Journal of Science, 2223–2239.
28. Laib, I., Mohammed, H. A., Laouini, S. E., Bouafia, A., Abdullah, M. M. S., Al-Lohedan, H. A., Al-Essa, Q., and Trzepieciński, T. (2025). Cutting-edge Nano-therapeutics: silver nanoparticles loaded with ciprofloxacin for powerful antidiabetic, antioxidant, anti-inflammatory, and antibiotic action against resistant pathogenic bacteria. International Journal of Food Science and Technology, vvaf024.
29. Alhujaily, M., Jabir, M. S., Nayef, U. M., Rashid, T. M., Sulaiman, G. M., Khalil, K. A. A., Rahmah, M. I., Najm, M. A. A., Jabbar, R., and Jawad, S. F. (2023). Au/ZnO Nanocomposites Prepared by Laser Ablation for Enhancement of Antibacterial Activity and Cytotoxic Properties against Cancer Cells. **Metals**, 13(4), 735.
30. Keskin, C., Aslan, S., Baran, M. F., Baran, A., Eftekhari, A., Adıcan, M. T., Ahmadian, E., Arslan, S., and Mohamed, A. J. (2025). Green synthesis and characterization of silver nanoparticles using anchusa officinalis: antimicrobial and cytotoxic potential. International Journal of Nanomedicine, 4481–4502.
31. Rauf, S., Hameed, H., Tariq, M., Afareen, A., Gulfaraz, S., AlKubaisi, N. A., and Elshikh, M. S. (2025). Phytochemical-Mediated Synthesis and Characterization of Silver Nanoparticles Using Mirabilis jalapa Leaf Extract and Their Antibacterial. Microscopy Research and Technique, 88(6), 1795–1805.
32. M07, C. (2024). Methods for Dilution Antimicrobial Susceptibility Tests for Bacteria That Grow Aerobically (12th ed.). Clinical and Laboratory Standards Institute.
33. Al-Dujaily, A. H., and Mahmood, A. K. (2022). Evaluation of Antibacterial and antibiofilm activity of biogenic silver nanoparticles and gentamicin against Staphylococcus aureus isolated from caprine mastitis. The Iraqi Journal of Veterinary

Medicine, 46(1), 10–16.
34. Azimzadeh, M., Greco, G., Farmani, A., Nourian, A., Pourhajibagher, M., Taherkhani, A., Alikhani, M. Y., and Bahador, A. (2025). Biofilm inhibition of multidrug-resistant Pseudomonas aeruginosa using green-synthesized silver nanoparticles and colistin. Scientific Reports, 15(1), 14993.
35. Ramezani, H., Sazegar, H., and Rouhi, L. (2025). The antimicrobial efficacy of rutin encapsulated chitosan versus multidrug-resistant Pseudomonas aeruginosa. Scientific Reports, 15(1), 22047.
36. George D, Mallery P. IBM SPSS statistics 26 step by step: A simple guide and reference. New York: Routledge; 2019.
37. Collee, J., Dugmid, J. P., Fraser, A., and Marmion, B. (1996). Practical medical microbiology, Mackie and Mc Cartney. Pearson professional limited. 14thed.
38. Lee, K.-S., and El-Sayed, M. A. (2006). Gold and silver nanoparticles in sensing and imaging: sensitivity of plasmon response to size, shape, and metal composition. The Journal of Physical Chemistry B, 110(39), 19220–19225.
39. Abdul Hussein, S. A., and Ghareeb, A. M. (2025). Assessment of efflux pump activity and screened the prevalence of associated genes Mex A and B among MDR Pseudomonas aeruginosa isolates.
40. AL-Rubaye, M. R. S., Mohammed, T. K., and Abdullah, H. N. (2020). Isolation and Diagnosis of Multi Drug Resistance Pseudomonas Aeruginosa from Wound and Burnpatients in Baghdad City. Indian Journal of Forensic Medicine and Toxicology, 14(3), 2431–2437.
41. Zainulabdeen, S. M. S. (n.d.). Bacteriological study for some aerobic bacteria contaminated the post–operative wounds.
42. Jangsangthong, A., Lugsomya, K., Apiratwarrasakul, S., and Phumthanakorn, N. (2024). Distribution of sequence types and antimicrobial resistance of clinical Pseudomonas aeruginosa isolates from dogs and cats visiting a veterinary teaching hospital in Thailand. BMC Veterinary Research, 20(1), 234.
43. Al-Saffar, M. F., and Jarallah, E. M. (2019). Isolation and characterization of Pseudomonas aeruginosa from Babylon province. Biochemical and Cellular Archives, 19(1).
44. Hasan, S. S., Said, L. A., and Hamed, S. L. (2020). Identification of clinical Pseudomonas spp. by VITEK 2 compact system and species-specific polymerase chain reaction assay for identification of Pseudomonas aeruginosa. J Drug Deliv Technol, 10(3), 383–388.
45. Robinson, V. H., Paterson, S., Bennett, C., and Steen, S. I. (2019). Biofilm production of Pseudomonas spp. isolates from canine otitis in three different enrichment broths. Veterinary Dermatology, 30(3), 218-e67.
46. Sharma, D., Pakravan, N., Pritchard, J. C., Hartmann, F. A., and Young, K. M. (2019). Mucoid Pseudomonas aeruginosa infection in a cat with severe chronic rhinosinusitis. Veterinary Clinical Pathology, 48(2), 300–304.
47. Milivojevic, D., Šumonja, N., Medić, S., Pavic, A., Moric, I., Vasiljevic, B., Senerovic, L., and Nikodinovic-Runic, J. (2018). Biofilm-forming ability and infection potential of Pseudomonas aeruginosa strains isolated from animals and humans. Pathogens and Disease, 76(4), fty041.
48. Adil, M., Alam, S., Amin, U., Ullah, I., Muhammad, M., Ullah, M., Rehman, A., and Khan, T. (2023). Efficient green silver nanoparticles-antibiotic combinations against antibiotic-resistant bacteria. AMB Express, 13(1), 115.
49. Todorova, M., Milusheva, M., Kaynarova, L., Georgieva, D., Delchev, V., Simeonova, S., Pilicheva, B., and Nikolova, S. (2023). Drug-loaded silver nanoparticles—a tool for delivery of a mebeverine precursor in inflammatory bowel diseases treatment. Biomedicines, 11(6), 1593.
50. Kamer, A. M. A., El Maghraby, G. M., Shafik, M. M., and Al-Madboly, L. A. (2024). Silver nanoparticle with potential antimicrobial and antibiofilm efficiency against multiple drug resistant, extensive drug resistant Pseudomonas aeruginosa clinical isolates. BMC Microbiology, 24(1), 277.